Available online at www.sciencedirect.com
ScienceDirect
Trans. Nonferrous Met. Soc. China 33(2023) 1792−1802
Transactions of Nonferrous Metals Society of China
www.tnmsc.cn

Effect of compositional homogenization on hot workability of Ni-based GH4061 superalloy

Guo-hua XU[1,2], Ran DUAN[1,2], Lei WANG[3], Yang LIU[3], Fan-qiang MENG[4]

1. Gaona Aero Material Co., Ltd., Beijing 100081, China;
2. Department of High-temperature Materials, Central Iron and Steel Research Institute, Beijing 100081, China;
3. Key Lab for Anisotropy and Texture of Materials, Ministry of Education, Northeastern University, Shenyang 110819, China;
4. Sino-French Institute of Nuclear Engineering and Technology, Sun Yat-Sen University, Zhuhai 519080, China

Received 21 December 2021; accepted 8 April 2022

Abstract: Complex solidification process, severe chemical segregation and large amounts of secondary phases with low melting point between dendrites deteriorate the hot workability of as-cast GH4061 superalloy. The effects of the homogenization temperature and time on the dendritic segregation, dissolution behavior of Laves phase with low melting point intermetallic phases and hot workability of the alloy were investigated using OM, SEM, EPMA and TEM. The results show that in the as-cast sample, severe compositional segregation is found among dendritic structures and the highest segregation coefficient of Nb is 2.435, followed by Ti of 1.346 and Mo of 1.200. After homogenization at 1160 °C for 20 h, the segregation among dendritic structures has been fully eliminated and the segregation coefficient of Nb declines to 1.098. Meanwhile, Laves and δ phases are mostly dissolved and no any localized grain boundary re-melting was observed. Increasing annealing temperature accelerates the speed of chemical homogenization and dissolution of intermetallic compounds. High-temperature mechanical properties testing results demonstrate that two-step homogenization treatment promotes the plasticity up to 1150 °C. Fracture analysis reveals that the dissolution of Laves and δ phases reduces the probability of crack initiation and fracture, resulting in a good hot workability.
Key words: GH4061 superalloy; dendritic segregation; Laves phase; hot workability

1 Introduction

Nickel-based superalloys are widely used in aero engines [1], industrial gas turbines [2] and high temperature nuclear power plant [3], because of their excellent mechanical properties, high-temperature creep properties and oxidation resistance [4]. In order to improve the mechanical properties at higher service temperatures, many elements, such as Mo, W, Nb, Ti and Al are added to enhance the solid solution and precipitation strengthening effects in superalloy [5]. On the other hand, the addition of so high number of strengthening solutes leads to the severe chemical segregation and formation of harmful intermetallics, thereby deteriorating the processability and mechanical performance at elevated temperatures [6,7]. Homogenization treatment plays a key role in eliminating segregation and obtaining homogenized microstructure so as to improve the formability of ingots for further processing or hot workability [8−11]. Optimizing homogenization parameters of Ni-based superalloys becomes more important task for the industrial applications [12−14].

Niobium (Nb) is an important strengthening element for wrought superalloys, which can concentrate in γ matrix, γ', γ'', δ phases and MC

Corresponding author: Lei WANG, Tel: +86-24-83681685, E-mail: wanglei@mail.neu.edu.cn;
Fan-qiang MENG, Tel: +86-18666112390, E-mail: mengfq5@mail.sysu.edu.cn
DOI: 10.1016/S1003-6326(23)66222-3

carbide [15]. MIGNANELLI et al [16] found that Nb addition is able to enhance the mechanical performance of superalloy via refining the γ' phase. Additionally, Nb was found to enhance the oxidation resistance of Ni-based superalloy through accelerating the formation of compact oxidation layer, which is able to inhibit the interdiffusion [4]. However, with increasing the Nb content, the segregation becomes serious and many detrimental phases are precipitated during solidification. PAN et al [17] reported that Nb was seriously segregated into the interdendritic regions with segregation coefficient as high as 4.30, accompanied by the formation of Nb-enriched phases including Laves phase, δ, MC and M_6C carbides in the as-cast GH742y alloy.

GH4061 superalloy is a highly alloyed Ni-based superalloy with total content of V, Mo, Nb and Al up to 9 wt.%, resulting in the formation of highly complicated precipitates, brittle intermetallics, as well as serious elemental segregations, which significantly degrade the hot workability [18]. However, the segregation behavior and the homogenization process in the large sized ingot have not been fully investigated. In the present study, the evolution of elemental segregation and microstructure of GH4061 ingot with a diameter of 508 mm was systemically investigated through undertaking heat treatments at different temperatures and holding time. The effect of homogenization treatment on the hot workability was studied by multi-scaled characterization methods and the fracture mechanism was discussed. A two-step homogenization treatment technology without incipient melting was established to eliminate the segregation and promote the higher plasticity at temperature up to 1150 °C.

2 Experimental

GH4061 ingot with a diameter of 508 mm used for the present investigation was prepared via vacuum induction melting plus vacuum arc re-melting. The overall chemical composition was measured using electron probe microanalysis (EPMA) and the result is listed in Table 1. Total content of Cr, Nb, Mo, Al, Fe, Ti and V additional elements is about 41.27 wt.%. In order to weaken the effect of the microstructural dependence on the location along the radial direction, all the samples for the current study were cut from the region about half radius to keep the results comparable. Homogenization heat treatment was carried out in muffle furnace at 1130, 1100, 1135, 1160, 1175, 1190, and 1200 °C in atmosphere for various holding time (1, 10 and 20 h), followed by water-quenching.

Table 1 Main chemical composition of as-cast GH4061 superalloy (wt.%)

Ni	Cr	Fe	Nb	Mo	Al	V	C	B
Bal.	17.78	13.45	4.87	4.00	1.17	0.44	0.028	0.0052

The microstructure characterization was carried out using confocal laser scanning microscope (VL2000DX−SVF17SP), scanning electron microscope (SEM, JEOL JSM−7800F) and transmission electron microscope (TEM, JEOL JEM−2100F). Elemental segregation and distribution were characterized using a JXA−8350F electron probe microanalyzer. Samples for optical microscope (OM) and SEM observations were mechanically ground, polished and electro-chemically etched. Gleeble tensile test was carried out at elevated temperatures with a constant strain rate of 0.1 s^{-1} to clarify the effect of homogenization on the mechanical properties and thermoplasticity. The sample with a gauge length of 10 mm and a diameter of 8 mm was heated up to the designed temperature with a constant heating rate of 10 °C/min, followed by isothermal holding for 60 s before testing. The fracture surface was characterized using SEM.

3 Results and discussion

3.1 Chemical segregation in as-cast sample

Chemical and microstructural variations are normally present in the large ingot, especially for the superalloys containing higher number of alloying elements, thus all the samples used for the following study were cut from the identical radius. Figure 1 shows the typical dendritic microstructure of as-cast GH4061 superalloy. The bright dendrite and black interdendritic regions shown in the longitudinal and transverse sections of as-cast sample (Figs. 1(a) and (b)) are typical structure of Ni-based superalloys [19]. SEM image with a large magnification (Fig. 1(c)) reveals the variation of phase configuration from dendritic core to inter-

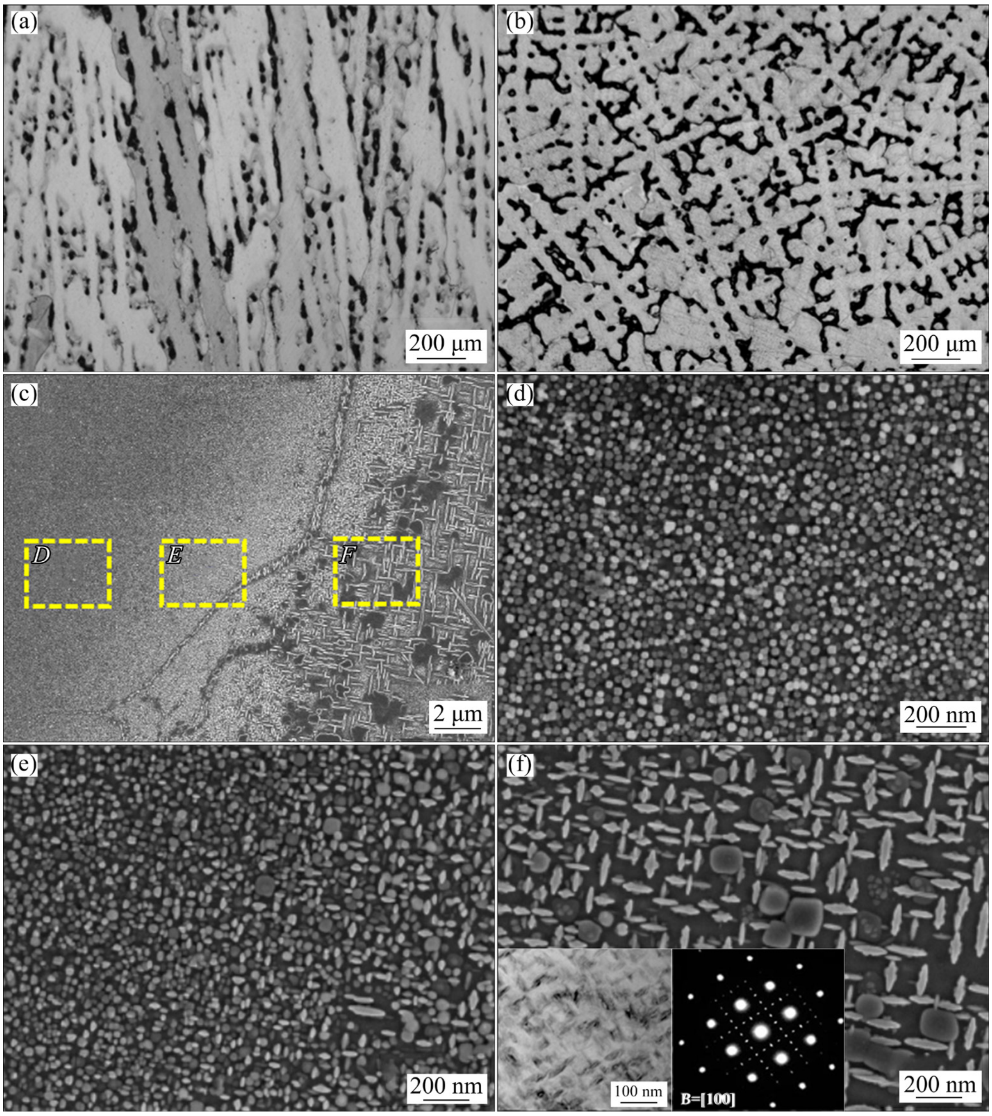

Fig. 1 OM images of longitudinal (a) and transverse (b) sections of as-cast GH4061 superalloy; SEM images (c−f) of dendritic structure with different kinds of precipitates γ' (d), $\gamma'+\gamma''$ (e) and γ'' (f) (The inset in (f) is TEM image of γ'' precipitates with corresponding selected area diffraction pattern)

dendritic region. Dendritic core (Region *D* marked in Fig. 1(c)) is mainly composed of the spherical γ' precipitates with an average diameter of 10−20 nm, while disc-shaped γ'' precipitates (Fig. 1(f)) are domain in the interdendritic region (Region *F* marked in Fig. 1(c)). Bright field TEM image and corresponding selected area diffraction pattern (inset in Fig. 1(f)) confirm that the disc-shaped γ'' precipitate is ordered bct (DO_{22}) Ni_3Nb, following the orientation relation with γ matrix: $(100)\gamma''//(100)\gamma$, $[001]\gamma''//\langle001\rangle\gamma$ [20]. A composite structure of γ' and γ'' (Fig. 1(e)) precipitates is shown in the transition region from dendritic core to interdendritic region (Area *E* marked in Fig. 1(c)).

It is known that dendritic phase solidifies firstly during the solidification and solutes are partitioned into the retained liquid, which finally transfer into interdendritic regions. Elemental mapping was carried out to clarify the distribution of solutes in the as-cast sample and the typical results are shown in Fig. 2. It can be seen that dendritic core is enriched by Fe, Cr and Al, while depleted by Ti, Mo and Nb. Interdendritic regions exhibit an opposite phenomenon. Thus, the purpose of homogenization treatment is to eliminate the segregation of Fe, Cr, Ti, Mo and Nb and obtain a uniform chemical composition. The point measurements were performed to evaluate the segregation degree and the calculated segregation

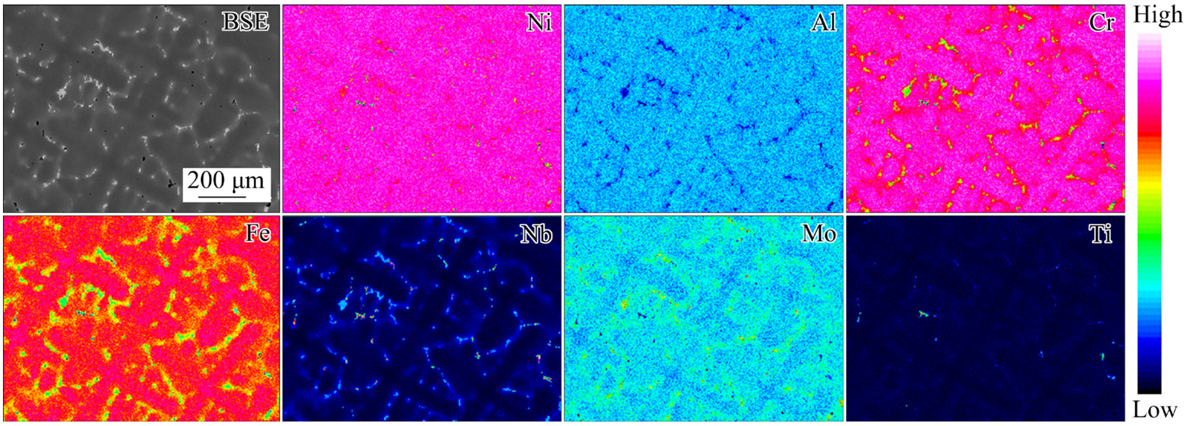

Fig. 2 Elemental distribution mapping of dendritic structure in as-cast sample

coefficients (K) of each alloying element between interdendritic region and dendritic core ($K=C^i_{\mathrm{inter}}/C^i_{\mathrm{core}}$, C^i_{inter} is the concentration of element i in interdendritic region, and C^i_{core} is the concentration of element i in dendritic core) are listed in Table 2 [21]. Nb owns the largest segregation coefficient of 2.435, followed by Ti of 1.346 and Mo of 1.200. The segregation coefficient of Nb, Ti and Mo is larger than 1, suggesting that these elements preferably segregate around interdendritic regions during solidification. In comparison, Fe and Cr with K less than 1 are enriched in dendritic cores, consisting with EDS mapping shown in Fig. 2.

Table 2 Segregation coefficient (K) of main alloying elements of GH4061 superalloy

Ti	Cr	Fe	Nb	Mo
1.346	0.901	0.859	2.435	1.200

Solutes are easily segregated around the interdendritic regions and grain boundaries, and preferably promote the formation of some complex phases and microstructure during solidification [22]. Figure 3(a) shows the representative SEM image of interdendritic region, where carbide (MC), Laves and δ phases are present. High magnification images shown in Figs. 3(b) and (c) reveal the island-shaped Laves and needle-shaped δ phase with an average length of 10−15 μm and the chemical analysis indicates that these δ particles are Ni_3Nb. However, the high volume fraction of intermetallics, i.e. MC, Laves and δ phases, are harmful to the mechanical properties and degrade the hot manufacturing abilities. DU et al [23] reported that tensile cracks tend to initiate at MC and Laves phase and then propagate along the phase boundary, resulting in the brittle fracture. Therefore, it is important to understand the chemical segregation trend and formation mechanism of brittle intermetallics. The representative elemental distribution mapping of Laves/γ structure is shown in Figs. 3(d−i). It is obvious that Nb and Mo are enriched heavily, while Al, Fe and Ni are depleted in Laves phase. Additionally, there are a few boride intermetallic compounds randomly distributed among Laves/γ eutectic structures. Previous works have reported that these boride phases do less impact on the mechanical properties due to the quite low volume fraction [23,24]. Therefore, the dissolution of boride phase is not discussed in the present study.

3.2 Compositional homogenization

The solidification simulation of GH4061 superalloy was carried out using the JmatPro software and the results indicated that liquidus temperature was 1361 °C, carbide formed at 1249 °C and Laves/γ eutectic phases formed at 1124 °C, and these results have been verified with microstructure observation by confocal laser microscopy (not shown). In order to eliminate the chemical segregation and dissolve all the intermetallic compounds, but avoid local re-melting of grain boundaries, a series of homogenization heat treatments were performed at different temperatures for different holding time to evaluate the proper parameters. The representative images shown in Fig. 4 demonstrate that either higher annealing temperature or longer holding time is

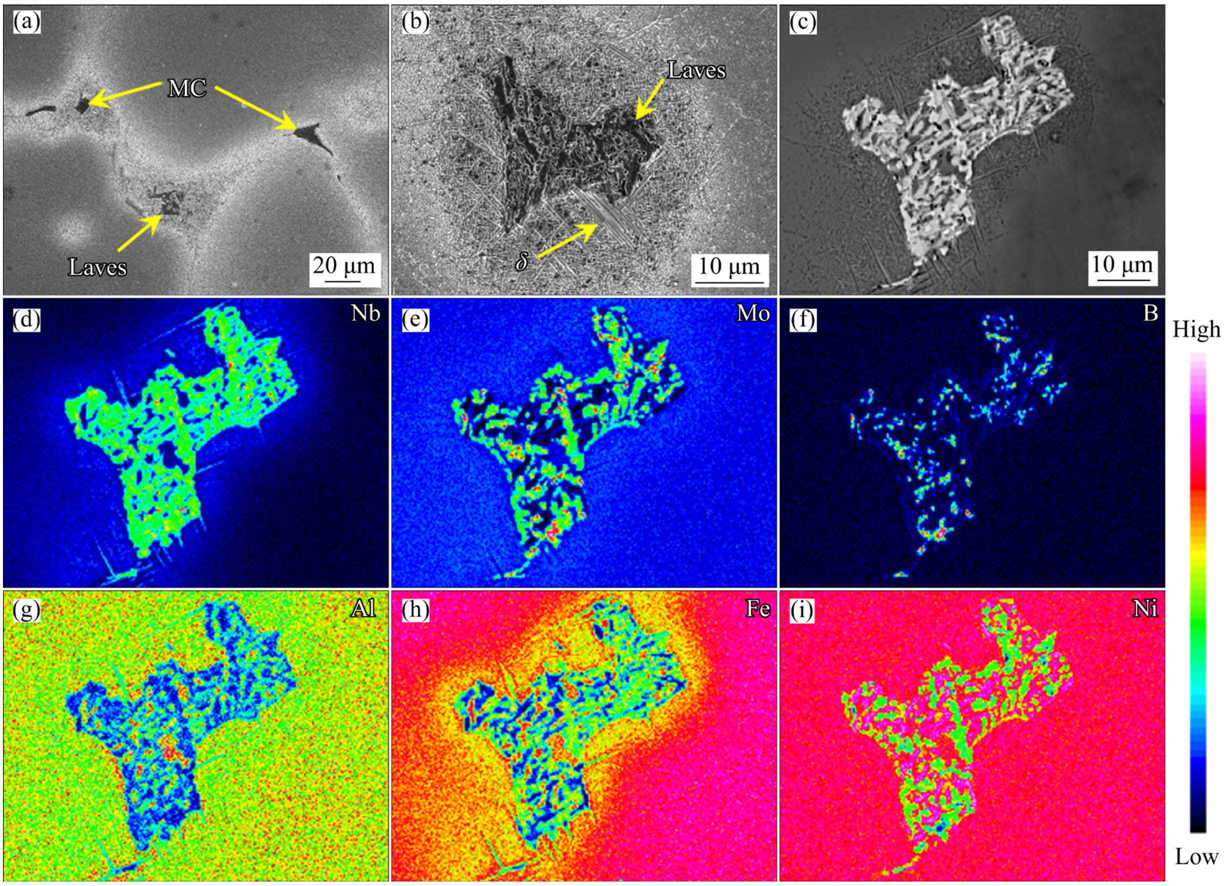

Fig. 3 SEM image of interdendrite region (a) and co-existence of Laves and δ phases (b), EPMA image (c) with corresponding elemental distributions of Nb (d), Mo (e), B (f), Al (g), Fe (h) and Ni (i)

beneficial to the dissolution of Laves and δ phases, but MC phase is still present even after annealing at 1200 °C for 20 h. Dissolution of MC usually requires even higher annealing temperature and longer holding time [25]. At lower temperature of 1100 °C, Laves and δ phases mostly dissolve after 20 h. In comparison, Laves/γ eutectic structures disappear after 10 h at 1160 °C and 1 h at 1200 °C. PAN et al [17] has reported that the interdiffusion coefficient of Nb at 1160 °C is two times higher than that at 1120 °C, thus increasing annealing temperature is an effective approach to decrease the segregation degree. Meanwhile, no any localized grain boundary re-melting is observed even annealing temperature up to 1200 °C for 20 h.

Elemental segregation in the dendritic region is very important for the mechanical properties. The evolution of elemental distribution was characterized using EPMA. Figure 5 shows the distribution of Nb among dendritic phases after different heat treatments. It is clearly shown that the higher homogenizing temperature and longer time accelerate the redistribution of Nb, eliminating the degree of segregation (uniform contrast in Fig. 5). In order to quantify the elemental segregation degree, the segregation coefficient was calculated based on the EPMA measurements, and the segregation coefficient variations of Ti, Fe, Cr, Nb and Mo are plotted as a function of annealing temperature and holding time (Figs. 6(a) and (b)). As the homogenizing time is fixed to be 20 h and annealing temperature varies from 1100 to 1200 °C, the lowest temperature to eliminate the chemical segregation is 1160 °C (Fig. 6(a)), where the segregation coefficients are close to 1 for most elements. When the temperature is fixed at 1160 °C, the segregation coefficient K continuously decreases with the increase of annealing time (Fig. 6(b)) and the shortest time of 10 h is needed to eliminate the elemental segregation. In Figs. 6(a) and (b), Nb exhibits the largest declining speed. The segregation coefficient of Nb declines to 1.098 after 20 h at 1160 °C. The lowest segregation coefficient of Nb is about 1.082 at 1200 °C for 20 h.

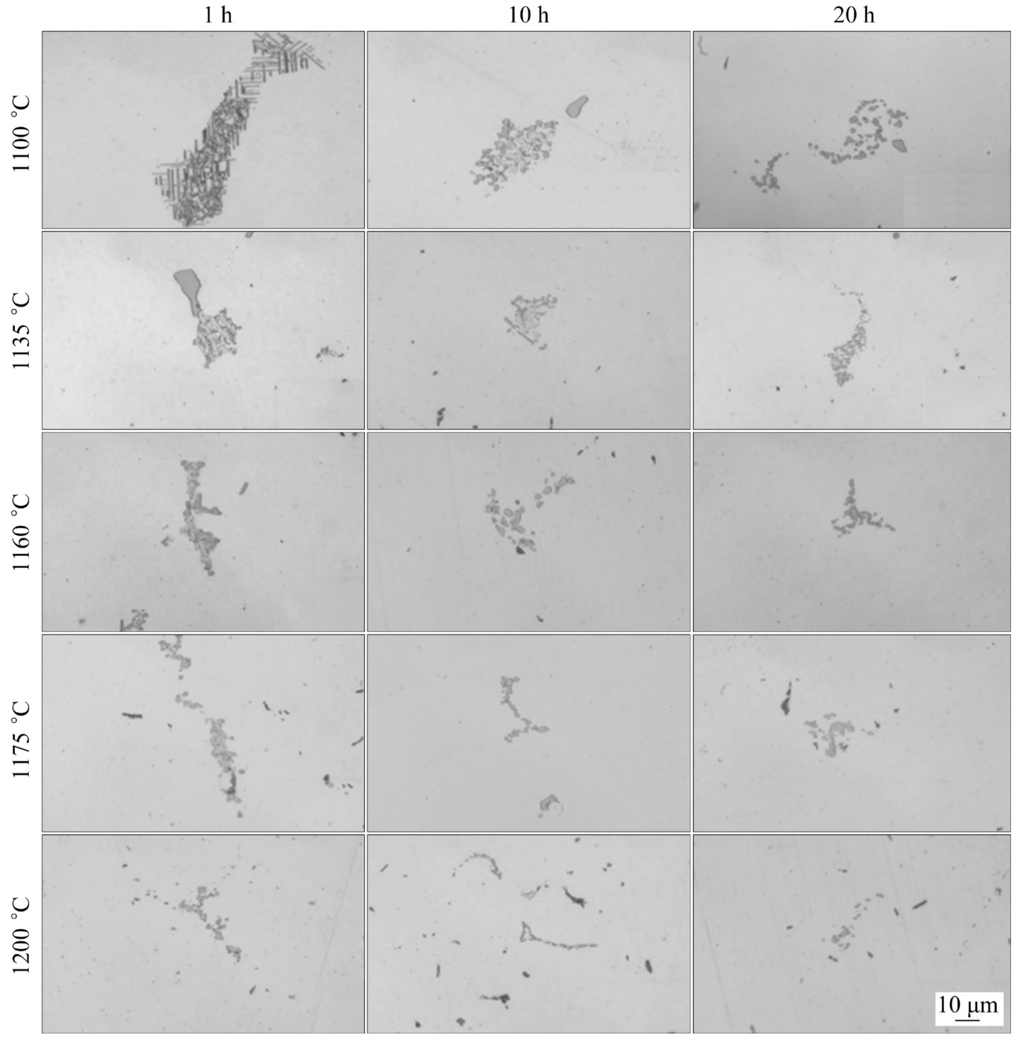

Fig. 4 Morphologies of Laves phases in annealed alloy samples at different temperatures and time

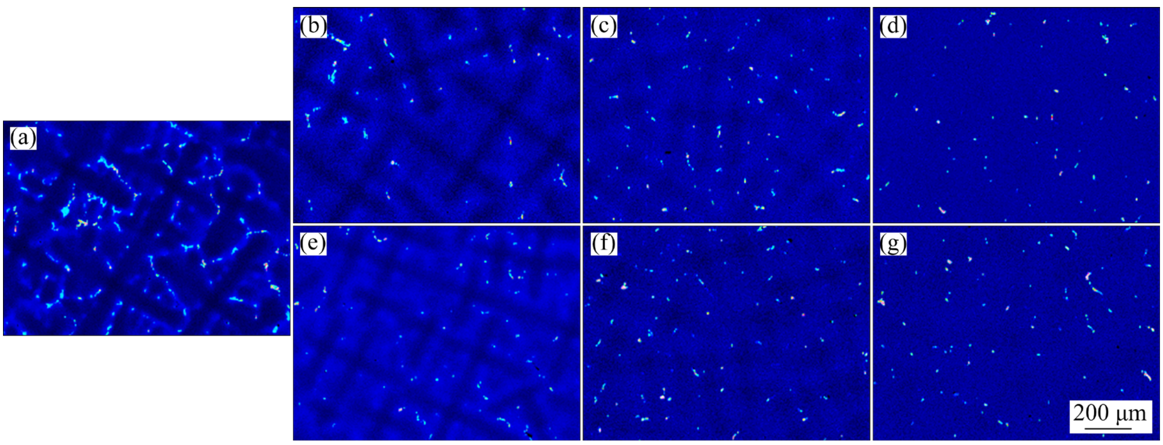

Fig. 5 EMPA mapping of Nb distribution in as-cast and different annealing treatment samples: (a) As-cast; (b) 1100 °C for 20 h; (c) 1135 °C for 20 h; (d) 1190 °C for 20 h; (e) 1160 °C for 1 h; (f) 1160 °C for 10 h; (g) 1160 °C for 20 h

In order to dissolve the Laves and δ phases as much as possible, two heat treatment processes were chosen to evaluate the effect of chemical homogenization on the mechanical properties. The first sample (HT1) was solution-treated at 1160 °C for 20 h and then at 1190 °C for 50 h, followed by furnace cooling. The second sample (HT2) was solution-treated at 1190 °C for 20 h and then at

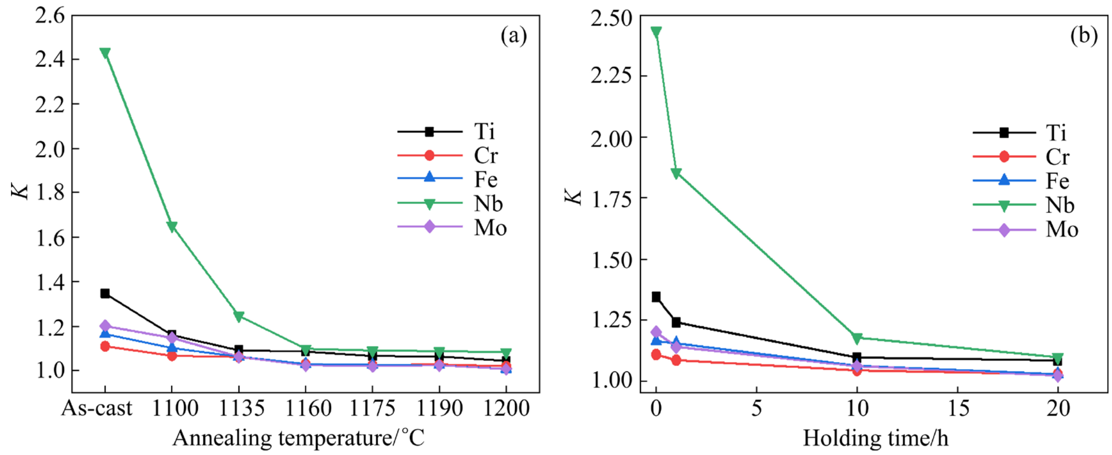

Fig. 6 Segregation coefficient variations of samples under different heat treatment conditions at different annealing temperatures for 20 h (a) and at 1160 °C for different holding time (b)

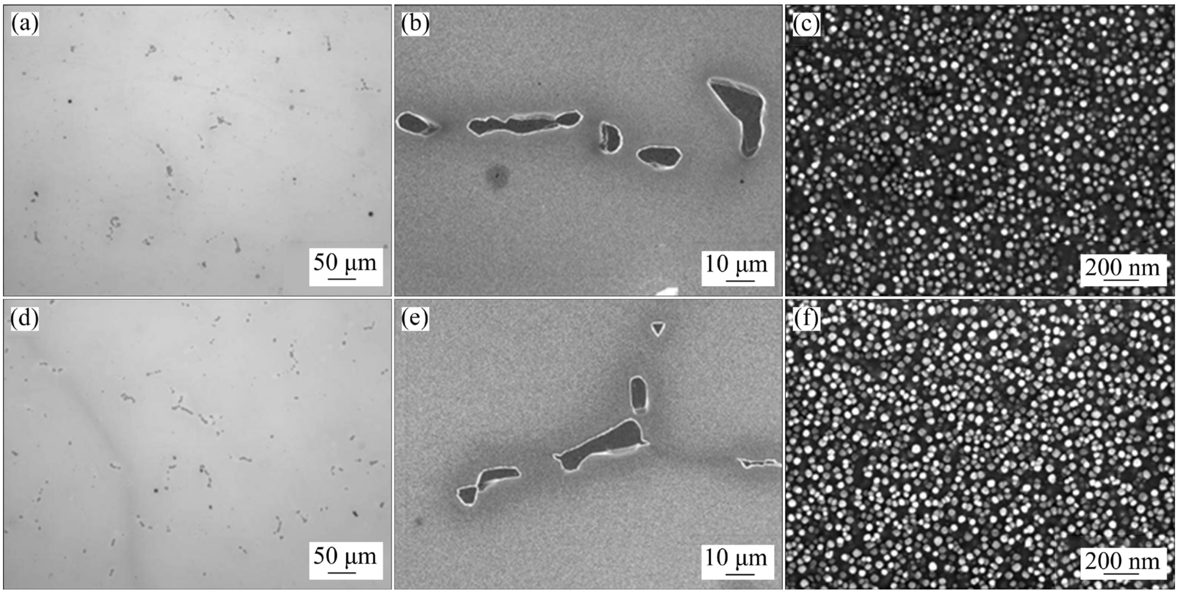

Fig. 7 OM (a, d) and SEM (b, c, e, f) images of HT1 (a−c) and HT2 (d−f) samples

1200 °C for 50 h, followed by furnace cooling. Microstructural difference between HT1 and HT2 processes is shown in Fig. 7. It can be seen that all the Laves/γ structure has been fully dissolved (Figs. 7(a) and (d)) and the retained particles are corresponding to MC. The morphologies of MC phase after two different heat treatments are shown in Figs. 7(b) and (c), which indicate that heat treatment parameters do not alter the size and distribution of MC phase obviously. Compared to the as-cast sample shown in Fig. 1(d), γ' particles become coarser and average diameter is about 40 nm in both HT1 and HT2 conditions (Figs. 7(c) and (f)). Additionally, EPMA measurements reveal that the chemical separation among the interdendritic regions and grain boundaries has been eliminated.

3.3 Mechanical properties at elevated temperature

The Gleeble hot tensile tests were carried out at four different temperatures (1050, 1100, 1150 and 1200 °C) and the mechanical properties are summarized in Fig. 8. It can be seen that the ultimate tensile strength (UTS) of both as-cast and homogenized samples decreases linearly with increasing temperature (Fig. 8(a)), while the reduction of cross-sectional area of homogenized samples nearly keeps stable as temperature is lower than 1200 °C compared to the as-cast one (Fig. 8(b)), suggesting that the workability at higher temperature has been improved. Both UTS and reduction of cross-sectional area of the samples after HT1 and HT2 heat treatments exhibit the similar trend, which are in agreement with the similar microstructure in Fig. 7. As the temperature approaches 1200 °C, reduction of cross-sectional area abruptly declines to zero in HT1 and HT2 samples, indicating the worst thermoplasticity. In comparison, the as-cast sample exhibits brittle failure when the temperature is higher than 1050 °C.

Fracture surface analysis demonstrates that the as-cast sample owns brittle feature (Fig. 9(a)) when the testing temperature is 1150 °C, and lots of Laves phases (Fig. 9(b)) are randomly distributed on the fracture plane. In comparison, the obvious necking feature appears in HT2 sample (Fig. 9(c)) coupled with a large number of dimples (Fig. 9(d)), suggesting the ductile fracture mode. Fracture induced by the retained MC phase in both HT1 and HT2 samples has not been found in the present study. However, SHENG et al [26] have reported that MC phase also contributes to the intermediate-temperature brittle structure in the directionally

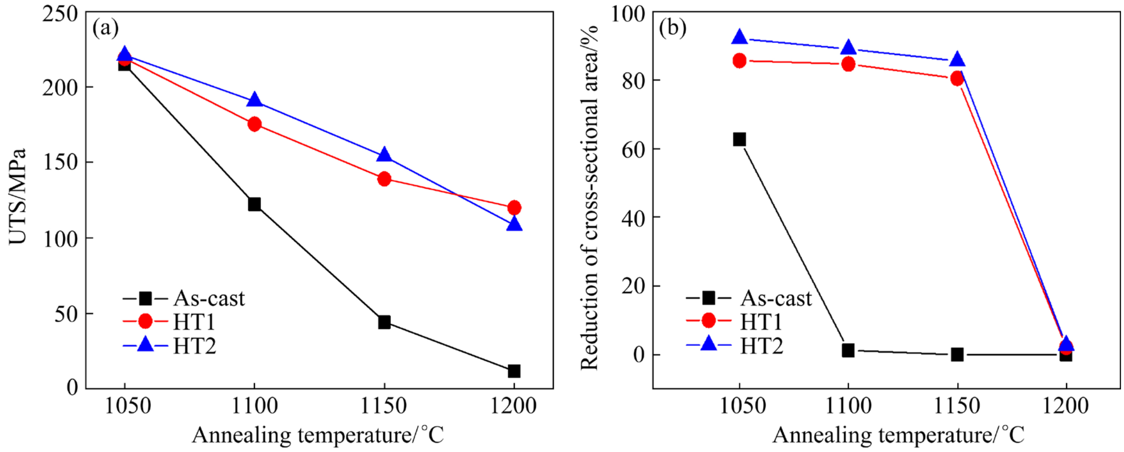

Fig. 8 Evolution of ultimate tensile strength (UTS) (a) and reduction of cross-sectional area (b) of as-cast and different heat-treated samples as function of annealing temperature

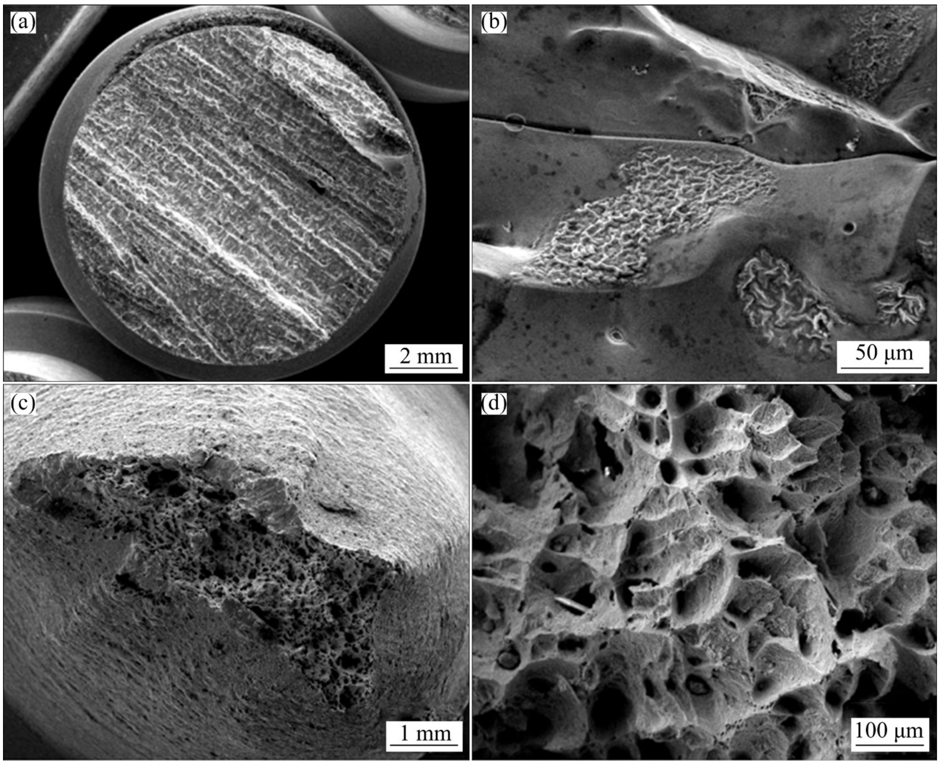

Fig. 9 Fracture surface morphologies of as-cast (a, b) and HT2 (c, d) samples tested at 1150 °C

solidified nick-based superalloy. The mechanical test and facture morphology analysis results demonstrate that the homogenization heat treatment promotes the workability at elevated temperature by eliminating the quenched-in chemical segregation and dissolving the brittle intermetallics, i.e. Laves and δ phases.

Elemental segregation is normally related to the competition between atomic diffusion and solidification speed, resulting in the formation of intermetallic compounds, i.e. Laves, MC, boride and δ phases. Under applied stress, the cracks are easily initiated at the interface between coarse intermetallic compounds and matrix due to different elastic moduli, leading to the brittle fracture and poor hot workability [23,27]. In the present study, the improvement of hot workability at elevated temperature is attributed to the dissolution of brittle δ phase, Laves phase and the reduction of the nucleation sites for cracks under stress. More uniform microstructure reduces the strain localization, contributing to the higher plasticity. On the other hand, the lower plasticity of the as-cast sample is also related to the Laves phase, which owns lower melting temperature of 1124 °C and can be possibly partially re-melted or softened at elevated temperature, leading to the earlier failure. Recently, SUI et al [28] have reported that the granular and sub-micron scale Laves phase can induce the formation of sub-grains (dislocation cells) and enhance the softening effect during high-temperature tests, while fine Laves phase is able to increase the alloy operating temperature. However, it has been proved that the coarse Laves/γ structure deteriorates the hot workability in the present study.

4 Conclusions

(1) Severe chemical segregation occurs in the as-cast GH4061 superalloy. Nb, Ti and Mo solutes are enriched in the interdendritic regions, in which high amount of Laves phase, MC and δ intermetallic compounds are present. The highest segregation coefficient of Nb is 2.435, followed by Ti of 1.346 and Mo of 1.200.

(2) The chemical segregation among dendritic structures has been fully eliminated after homogenization at 1160 °C for 20 h and the segregation coefficient of Nb also declines to 1.098. Meanwhile, Laves and δ phases are mostly dissolved after 10 h at 1160 °C, but MC phase, owning higher dissolution temperature, is still retained even after being annealed at 1200 °C for 20 h.

(3) The elimination of chemical segregation and dissolution of brittle intermetallic compounds through two-step homogenization treatment remarkably improve the plasticity up to 1150 °C. In comparison, the as-cast sample exhibits a brittle failure as testing temperature is higher than 1050 °C. The improvement of workability at elevated temperatures is attributed to the reduction of nucleation sites for cracks and fracture via homogenization treatment.

Acknowledgments

This research was financially supported by the National Natural Science Foundation of China (Nos. U1708253, 52271126) and the Major Projects in Aviation Engines and Gas Turbines, China (No. 2017-VI-0002-0071, 2019-VI-0020-0136). Fan-qiang MENG acknowledges the financial support from the National Center for Materials Service Safety Foundation, China.

References

[1] BOYD-LEE A D. Fatigue crack growth resistant microstructures in polycrystalline Ni-base superalloys for aeroengines [J]. International Journal of Fatigue, 1999, 21(4): 393−405.

[2] OKAZAKI M. High-temperature strength of Ni-base superalloy coatings [J]. Science and Technology of Advanced Materials, 2001, 2(2): 357−366.

[3] TAN L, REN X, SRIDHARAN K, ALLEN T R. Corrosion behavior of Ni-base alloys for advanced high temperature water-cooled nuclear plants [J]. Corrosion Science, 2008, 50(11): 3056−3062.

[4] YE Xian-jue, YANG Biao-biao, NIE Yan, YU Shu, LI Yun-ping. Influence of Nb addition on the oxidation behavior of novel Ni-base superalloy [J]. Corrosion Science, 2021, 185: 109436.

[5] MANIKANDAN S G K, SIVAKUMAR D, RAO K P, KAMARAJ M. Effect of weld cooling rate on Laves phase formation in Inconel 718 fusion zone [J]. Journal of Materials Processing Technology, 2014, 214(2): 358−364.

[6] BARBA D, SMITH T M, MIAO J, MILLS M J, REED R C. Segregation-assisted plasticity in Ni-based superalloys [J].

Metallurgical and Materials Transactions A, 2018, 49(9): 4173−4185.

[7] BIAN Hua-kang, CUI Yu-jie, LI Yun-ping, CHIBA A, NIE Yan. The influence of Mo on Suzuki-segregation-related microstructure evolution and mechanical properties of Co−Ni-based superalloy [J]. Journal of Alloys and Compounds, 2018, 768: 136−142.

[8] LIU J L, MENG J, YU J J, ZHOU Y Z, SUN X F. Influence of solidification conditions and alloying elements Re and Ti on micropores formed during homogenization of Ni base single crystal superalloy [J]. Journal of Alloys and Compounds, 2018, 746: 428−434.

[9] HOSSEINI S A, MADAR K Z,ABBASI S M. Effect of homogenization heat treatments on the cast structure and tensile properties of nickel-base superalloy ATI 718Plus in the presence of boron and zirconium additions [J]. Materials Science and Engineering A, 2017, 689: 103−114.

[10] BOKSTEIN B S, EPISHIN A I, LINK T, ESIN V A, RODIN A O, SVETLOV I L. Model for the porosity growth in single-crystal nickel-base superalloys during homogenization [J]. Scripta Materialia, 2007, 57(9): 801−804.

[11] YANG Fei, HOU Jie-shan, WANG Chang-shuai, ZHOU Lan-zhang. Effects of solution treatment on microstructure and tensile properties of as-cast alloy 625 [J]. Transactions of Nonferrous Metals Society of China, 2021, 31(2): 426−437.

[12] LI Yi-ling, JIA Zhi-hong, TANG Wei, LIANG Xiang-feng, XU Wei-tai, ZHAO Yu-tao. Changes in the diffusion coefficient of rhenium in a new type of nickel-based single-crystal superalloy during homogenization [J]. Advanced Engineering Materials, 2020, 22(4): 1901151.

[13] CUI Hong-yang, TAN Yi, BAI Ru-sheng, LI Yi, ZHUANG Xin-peng, CHEN Zi-ang, YOU Xiao-gang, LI Peng-ting, CUI Chuan-yong. Microsegregation of a new Ni−Co-based superalloy prepared by electron beam smelting layered solidification technology and its homogenization behavior [J]. Materials Characterization, 2022, 184: 111668.

[14] TAN Gang, LI Hui-zhong, WANG Yan, YANG Lei, QIAO Shi-chang, HUANG Zheng-qin, LIU Min-xue. Hot working characteristics of HEXed PM nickel-based superalloy during hot compression [J]. Transactions of Nonferrous Metals Society of China, 2020, 30(10): 2709−2723.

[15] SMITH G D, PATEL S J. The role of niobium in wrought precipitation-hardened nickel-base alloys [J]. Superalloys, 2005, 718: 625−706.

[16] MIGNANELLI P M, JONES N G, HARDY M C, STONE H J. The influence of Al:Nb ratio on the microstructure and mechanical response of quaternary Ni−Cr−Al−Nb alloys [J]. Materials Science and Engineering A, 2014, 612(26): 179−186.

[17] PAN Xiao-lin, YU Hai-yan, TU Gan-feng, SUN Wen-ru, HU Zhuang-qi. Segregation and diffusion behavior of niobium in a highly alloyed nickel-base superalloy [J]. Transactions of Nonferrous Metals Society of China, 2011, 21(11): 2402−2407.

[18] HUANG Shuo, HE Yu-wei, XU Guo-hua, DUAN Ran, WANG Lei, ZHAO Guang-pu. Effects of vanadium on microstructure and mechanical properties of a wrought nickel-based superalloy [J]. Chinese Journal of Materials Research, 2019, 33(6): 419−426. (in Chinese)

[19] GONG Li, CHEN Bo, DU Zhan-hui, ZHANG Meng-shu, LIU Rui-chang, LIU Kui. Investigation of solidification and segregation characteristics of cast Ni-base superalloy K417G [J]. Journal of Materials Science & Technology, 2018, 34(3): 541−550.

[20] HONG S J, CHEN W P, WANG T W. A diffraction study of the γ'' phase in INCONEL 718 superalloy [J]. Metallurgical and Materials Transactions A, 2001, 32(8): 1887−1901.

[21] MIAO Zhu-jun, SHAN Ai-dang, WU Yuan-biao, LU Jun, XU Wen-liang, SONG Hong-wei. Quantitative analysis of homogenization treatment of INCONEL718 superalloy [J]. Transactions of Nonferrous Metals Society of China, 2011, 21(5): 1009−1017.

[22] WANG Jian, ZHOU Lan-zhang, SHENG Li-yuan, GUO Jian-ting. The microstructure evolution and its effect on the mechanical properties of a hot-corrosion resistant Ni-based superalloy during long-term thermal exposure [J]. Materials & Design, 2012, 39: 55−62.

[23] DU Bei-ning, HU Zi-yang, SHENG Li-yuan, CUI Chuan-yong, YANG Jin-xia, ZHENG Yu-feng, SUN Xiao-feng. Tensile, creep behavior and microstructure evolution of an as-cast Ni-based K417G polycrystalline superalloy [J]. Journal of Materials Science & Technology, 2018, 34(10): 1805−1816.

[24] HU X B, ZHU Y L, SHENG N C, MA X L. The Wyckoff positional order and polyhedral intergrowth in the M3B2- and M5B3-type boride precipitated in the Ni-based superalloys [J]. Scientific Reports, 2014, 4(1): 7367.

[25] LVOV G, LEVIT V I, KAUFMAN M J. Mechanism of primary MC carbide decomposition in Ni-base superalloys [J]. Metallurgical and Materials Transactions A, 2004, 35(6): 1669−1679.

[26] SHENG Li-yuan, YANG Fang, GUO Jian-ting, XI Ting-feng. Anomalous yield and intermediate temperature brittleness behaviors of directionally solidified nickel-based superalloy [J]. Transactions of Nonferrous Metals Society of China, 2014, 24(3): 673−681.

[27] FAYED E M, SAADATI M, SHAHRIARI D, BRAILOVSKI V, JAHAZI M, MEDRAJ M. Effect of homogenization and solution treatments time on the elevated-temperature mechanical behavior of Inconel 718 fabricated by laser powder bed fusion [J]. Scientific Reports, 2021, 11(1): 2020.

[28] SUI Shang, LI Zuo, ZHONG Chong-liang, ZHANG Qiang, GASSER A, CHEN Jing, CHEW You-xiang, BI Gui-jun. Laves phase tuning for enhancing high temperature mechanical property improvement in laser directed energy deposited Inconel 718 [J]. Composites (Part B): Engineering, 2021, 215: 108819.

均匀化处理工艺对镍基 GH4061 高温合金热加工性能的影响

胥国华[1,2]，段 然[1,2]，王 磊[3]，刘 杨[3]，孟凡强[4]

1. 北京钢研高纳科技股份有限公司，北京 100081；
2. 钢铁研究总院 高温材料研究所，北京 100081；
3. 东北大学 材料各向异性与织构教育部重点实验室，沈阳 110819;
4. 中山大学 中法核工程与技术学院，珠海 519080

摘 要：针对镍基 GH4061 高温合金凝固过程复杂、铸态组织偏析严重、枝晶间生成的大量低熔点第二相、严重降低合金的热加工性能的问题，采用 OM、SEM、EPMA 和 TEM 系统研究均匀化处理温度和时间对 GH4061 合金枝晶偏析、低熔点 Laves 相等回溶行为及合金热加工性能的影响。结果表明，铸态合金中发生严重的枝金偏析，Nb、Ti 和 Mo 元素枝晶间偏析系数分别高达 2.435、1.346 和 1.200。经 1160 ℃保温 20 h 均匀化处理后，枝金偏析得到充分消除，Nb 元素枝晶间偏析系数降低到 1.098；同时，Laves 和 δ 相基本回溶，且无晶界熔化现象；提高热处理温度显著加速成分均匀化与低熔点第二相的回溶速度。高温力学性能研究结果表明，两级均匀化热处理能够有效地提高合金热加工塑性至 1150 ℃；断口分析表明，低熔点的 Laves 相和 δ 相的回溶降低了裂纹萌生与断裂的几率，提高了合金的塑性变形能力。

关键词：GH4061 高温合金；枝晶偏析；Laves 相；热加工性能

(Edited by Wei-ping CHEN)